JOURNAL OF MORPHOLOGY 243:113–126 (2000)

Stiffening the Stingray Skeleton — An Investigation of Durophagy in Myliobatid Stingrays (Chondrichthyes, Batoidea, Myliobatidae)

Adam P. Summers*

Organismic and Evolutionary Biology, University of Massachusetts, Amherst, Massachusetts

ABSTRACT The stingray family Myliobatidae contains five durophagous (hard prey specialist) genera and two planktivorous genera. A suite of morphological features makes it possible for the hard prey specialists to crush mollusks and crustaceans in their cartilaginous jaws. These include: 1) flat, pavement-like tooth plates set in an elastic dental ligament; 2) multiple layers of calcified cartilage on the surface of the jaws; 3) calcified struts running through the jaws; and 4) a lever system that amplifies the force of the jaw adductors. Examination of a range of taxa reveals that the presence of multiple layers of calcified cartilage, previously described from just a few species, is a plesiomorphy of Chondrichthyes. Calcified struts within the jaw, called "trabecular cartilage," are found only in the myliobatid genera, including the planktivorous *Manta birostris*. In the durophagous taxa, the struts are concentrated under the area where prey is crushed, thereby preventing local buckling of the jaws. Trabecular cartilage develops early in ontogeny, and does not appear to develop as a direct result of the stresses associated with feeding on hard prey. A "nutcracker" model of jaw function is proposed. In this model, the restricted gape, fused mandibular and palatoquadrate symphyses, and asynchronous contraction of the jaw adductors function to amplify the closing force by 2–4 times. J. Morphol. 243:113–126, 2000.

KEY WORDS: hard prey; cartilage; calcification; ontogeny; jaws; feeding

Cartilaginous fishes manage to fill many of the same niches as bony fishes in spite of a skeleton that is neither as stiff nor as strong as one made of bone. Among the cartilaginous fishes there are sharks capable of swimming 60 km/h (Compagno, 1984), giants weighing over 10 metric tons (Gudger, 1915), and hard prey specialists capable of crushing crabs, snails, and mussels (Gudger, 1914; Smith, 1942). These functional extremes show that, although cartilage is not as stiff or as strong as bone, it is able to perform under physically demanding stress regimes. Durophagous chondrichthians, which specialize in crushing hard prey, are a particularly intriguing example, illustrating the demands placed on the cartilaginous skeleton. How can cartilaginous jaws be used to crush prey that is harder than the jaws themselves?

Durophagy has been studied in many groups of vertebrates, including bony fish (e.g., Wainwright, 1987; Norton, 1988; Turingan and Wainwright, 1993), reptiles (e.g., Gans, 1952; Herrel et al., 1997; Lappin, 1997), birds (e.g., Homberger and Brush, 1986; Homberger, 1988; Gosner, 1993), and mammals (e.g., Rensberger and Stefen, 1995; Biknevicius, 1996). A number of morphological features are associated with eating hard prey, including heavy, pavement-like dentition, large jaw adductors, and jaws made of stiff, strong bone. Bone, the usual structural material of vertebrates, is stiffened in two ways, either by cortical thickening or by trabeculation. Cortical thickening is the endosteal and periosteal deposition of mineral, resulting in a thicker layer of bone around the marrow cavity. Trabeculation is the formation of mineralized struts within the marrow cavity of a bony element which transfer and dissipate forces applied to the cortical layer (Thompson, 1917; Swartz et al., 1998).

Cartilaginous analogs of both these methods of strengthening bone have been briefly reported on in a durophagous stingray (Summers et al., 1998). These cartilaginous analogs are variations on the usual mode of endoskeletal calcification in cartilaginous fishes. The cartilaginous skeleton of the Chondrichthyes is primarily composed of hyaline cartilage, partially calcified, with a thin surface rind of "prismatic cartilage" divided into mineralized blocks, called "tesserae" (Ørvig, 1951; Moss, 1977; Clement, 1986). This tesserate prismatic cartilage is a synapomorphy of the cartilaginous fishes (Smith

Contract grant sponsor: the National Science Foundation; Contract grant number: IBN 9801636; Contract grant sponsor: the Organismic and Evolutionary Biology Program at the University of Massachusetts.

*Correspondence to (new address): Adam P. Summers, Museum of Vertebrate Zoology - 3101 VLSB, UC Berkeley, Berkeley, CA 94720-3160. E-mail asummers@uclink.berkeley.edu

and Hall, 1990). A typical skeletal element has a fibrous outer perichondral layer with spindle-shaped fibroblasts. Under this perichondrium lies a single layer of calcified tesserae. Fibroblasts at the interface of the perichondrium and the tesserae may initiate calcification, depositing mineral on the outer surface of developing tesserae. Collagenous fibers (Sharpey's fibers) anchor the perichondrium to the underlying calcified cartilage (Kemp and Westrin, 1979). Beneath the layer of tesserae is a core of hyaline cartilage. As is typical of cartilage, there is no vascular supply for the chondrocytes maintaining the extracellular matrix (ECM); nutrients, hormones, and minerals must reach the chondrocytes by diffusion.

The cartilaginous analog of cortical thickening is the deposition of either thicker or more numerous layers of tesserae on the surface of a skeletal element. There are several examples of the latter type of reinforcement. Multiple layers of tesserae were first described from fossil xenacanthine sharks (Schaeffer, 1981). This was considered an anomaly that could shed light on the process of mineralization, but only if there were living taxa that exhibited similar morphology. Multiple layers of tesserae have been found in the jaws of extant sharks (Dingerkus et al., 1991); however, they were thought to be restricted to the jaw joints of very large individuals of just a few species. Examination of the jaws of the cownose ray revealed that they too exhibit multiple layers of tesserae, in this case covering most of the jaw surface (Summers et al., 1998).

The cartilaginous analog to trabeculation is mineralized struts running through the hyaline cartilage core of a skeletal element. The existence of this form of calcified cartilage, called "trabecular cartilage," has been documented in cownose rays (Summers et al., 1998), although the histology, ontogeny, and phylogenetic distribution is described briefly or not at all. The struts appear to be hollow elements passing all the way through the jaw. The walls of the hollow struts are composed of calcified blocks of cartilage that closely resemble the tesserae of the surface calcification.

Durophagy evolved in at least three different clades of cartilaginous fishes: holocephalans (chimaeroids) (Dean, 1906), heterodontids (horn sharks) (Smith, 1942) and stingrays of the family Myliobatidae (Bigelow and Schroeder, 1953). Myliobatids are members of the Batoidea, a clade of dorsoventrally flattened elasmobranchs, derived from sharks, united by a number of characters, including an upper jaw (palatoquadrate) without skeletal or ligamentous connection to the chondrocranium (McEachran et al., 1996). The typical batoid jaw, as exemplified by a dasyatid stingray (Fig. 1), is particularly poorly designed for durophagy. The left and right sides of both the upper and lower jaw are not well joined and the teeth are small and sharply pointed. The independence of the left and right sides of the jaws allows exceptional freedom of movement.

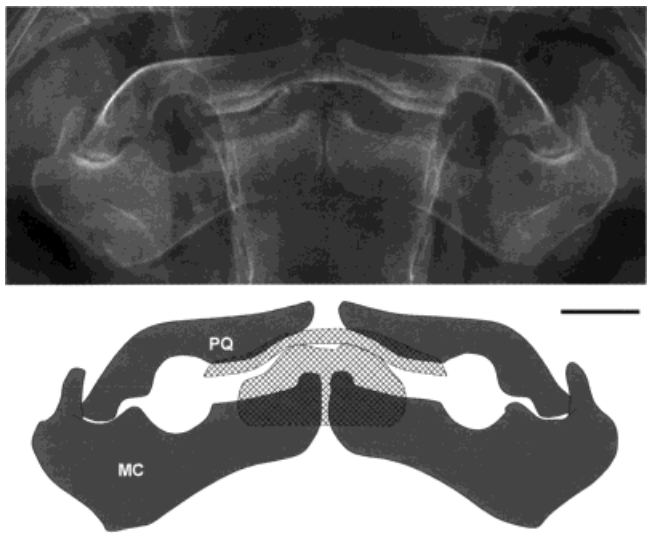

Fig. 1. Radiograph and tracing of the jaws and teeth of a southern stingray, *Dasyatis sabina,* in dorsoventral projection. An uncalcified central region of cartilage and ligament separates the calcified left and right sides of Meckel's cartilage (MC) and the palatoquadrate (PQ). The southern stingray eats primarily soft-bodied benthic invertebrates and fish (Rasmussen and Heard, 1995). The position of the teeth is indicated with hatching. Scale bar = 1 cm.

Cinevideography of a stingray (*Dasyatis sabina*) showed independent motion of the sides of the jaws during prey processing (Summers, 1995); however, it is not suited to exerting the large forces needed for crushing hard prey.

Myliobatid stingrays are a particularly interesting group in which to examine the evolution of morphological novelties associated with eating hard prey. The family Myliobatidae (sensu Nishida, 1990) is a clade of pelagic stingrays with worldwide distribution. Of the seven genera in the family, five are hard prey specialists (*Rhinoptera, Myliobatis, Pteromylaeus, Aetomylaeus* and *Aetobatus*), and two (*Manta* and *Mobula*), are planktivores (Bigelow and Schroeder, 1953; Wallace, 1967; Last and Stevens, 1994). The currently accepted phylogenetic hypothesis of the relationships among batoid fishes suggests that durophagy evolved at the base of the myliobatid clade and has been lost in the planktivorous genera (Nishida, 1990; Lovejoy, 1996; McEachran et al., 1996). In addition to the comparison between durophagy and planktivory within the family, myliobatids can be compared with numerous outgroup taxa, ranging from other stingrays to sharks, which eat soft prey.

The goals of this study were: 1) to describe the morphology of the jaws of durophagous stingrays; 2) to provide further description of trabecular cartilage; 3) to illustrate the ontogeny of trabecular cartilage and the morphology of the jaws; 4) to determine the phylogenetic extent of multiple layers of prismatic cartilage and trabecular cartilage; and 5)

to provide a testable model of the function of the jaw morphology.

MATERIALS AND METHODS

Animals

Fourteen cownose rays, *Rhinoptera bonasus*, ranging from 56 cm disk width (DW) adults to a 21 cm DW aborted embryo, were captured using hook and line, gill nets, and hand nets in Tampa Bay, Florida, and Beaufort, North Carolina. Other species of elasmobranch were collected in Tampa Bay by hook and line and dip net for comparative purposes, including guitarfish, *Rhinobatos lentiginosus* (n = 1), Atlantic stingrays, *Dasyatis sabina* (n = 5), and short nose stingrays, *Dasyatis sayi* (n = 3). Specimens were kept on ice until returned to the lab. Eight fresh-frozen heads of the spotted eagle ray, *Aetobatus narinari,* were obtained from commercial fisherman in Puerto Rico. Further material, either preserved in alcohol or dried, was obtained from the fish collections at the Museum of Comparative Zoology (MCZ) at Harvard University and the University of Massachusetts Museum of Natural History in Amherst, MA.

Radiography

Radiographs of fresh and frozen material from *Rhinoptera bonasus* (n = 9), *Rhinobatos lentiginosus* (n = 1), *Dasyatis sayi* (n = 1), and *D. sabina* (n = 2) were made on Kodak X-OMAT AR film using a Hewlett-Packard cabinet X-ray system (Faxitron model #43855A) and processed with an automated processor. A band saw, with the guide fence set to cut 1–3 mm thick pieces, was used to make sagittal and transverse sections of whole, frozen animals that were then radiographed. The tooth plates were removed from the jaws of three cownose rays and one eagle ray. These jaws were radiographed without the tooth plates, sectioned on the band saw, and radiographed again. A computed axial tomography (CAT) scanner and three-dimensional reconstruction software were used to examine the anatomy of the calcified tissue of *R. bonasus* and *Aetobatus narinari.* The jaws of one individual each of *Taeniura lymma, Gymnura altivela, Urolophus jamaicensis, Raja erinacea, R. ocellata,* and *Myliobatis californicus* were examined with a Siemens cineradiograph in fluoroscope mode. Measurements of the trabeculae were made directly from the radiographs on a light box with a digital hand caliper.

Histology

The jaws of a fresh, unfrozen cownose ray and the head of a southern stingray were removed and cut into blocks with a heavy scalpel. These blocks were preserved in 3% neutral buffered formalin for 48 h, then decalcified in a formic acid/sodium citrate solution for 72 h before embedding in paraffin. Sections were cut at 10 microns on a Reichert-Jung flatbed microtome and stained with either hemotoxylin/eosin, Mallory's triple stain, Masson's trichrome, or Alcian blue/Van Gieson (pH 2.5) according to methods described in Humason (1972). Sections were examined and photographed with a Nikon Optiphot using ordinary light, differential interference contrast, and polarized light. Wide field views were obtained with a Nikon stereomicroscope and a Pixera digital camera. Additionally, a large, wedge-shaped section (3 cm), removed from the lower jaw of an adult manta ray with a scalpel was examined under a Zeiss stereomicroscope.

Other Methods

Fresh and preserved cownose rays (4), spotted eagle rays (4), southern stingrays (2), and a short nose stingray (1) were dissected and manipulated to test hypotheses regarding jaw architecture and function. To confirm the mineralization pattern shown by the radiographs, thick sections (3 mm) of cownose ray jaws were stained with Alizarin Red S and cleared in KOH and glycerin. A 4 mm wide sagittal section was sawn from the tooth plates from the largest spotted eagle ray head. The section was broken into 2 cm pieces, embedded in epoxy, and ground flat for examination with a Cameca SX50 Electron Microprobe to determine the elemental composition of the teeth.

Disposition of Material Examined

Most of the fresh material in this study was discarded after examination for logistical reasons. Specimens examined at the MCZ include: *Gymnura altivela* (MCZ40731, 330 mm TL), *Hydrolagus collei* (MCZ147445, 460 mm TL), *Manta birostris* (MCZ 37006, unknown size and sex; MCZ-1111, embryo), *Myliobatis californicus* (MCZ36467, 380 mm TL), *Pristis pectinatus* (MCZ-1221, saw; MCZ89872, saw), *Raja erinacea* (MCZ100484, 500 mm TL), *Raja ocellata* (MCZ100488, 630 mm TL), *Taeniura lymna* (MCZ40480), *Urolophus jamaicensis* (MCZ51944, 293 mm TL). Specimens at the University of Massachusetts Museum of Natural History include *Aetobatus narinari* (UMA-0035, jaws).

RESULTS

Jaws and Teeth

The jaws of all of the myliobatid stingrays examined in this study are far more robustly constructed than the jaws of other batoid fishes. The mandibular symphysis is entirely fused, as is the palatoquadrate symphysis, and the jaws themselves are comparatively larger than those of other stingrays (Fig. 2). F2
Two thick, parallel-fibered ligaments limit the relative mobility of the upper and lower jaws to just two degrees of freedom. Gross manipulation reveals that

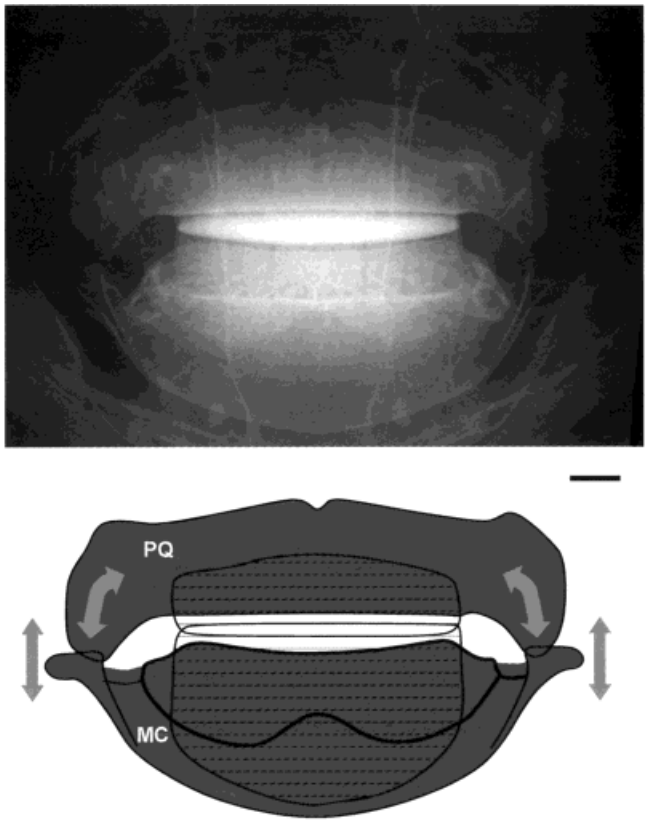

Fig. 2. Radiograph and tracing of the jaws and tooth plates of a hard-prey specialist, the cownose ray *Rhinoptera bonasus*, in dorsoventral projection. Note the fully calcified symphyses in both the upper and lower jaws. The jaws can move relative to one another only in the plane of the page, as shown by the arrows. All other movements are constrained by ligaments at the jaw joint. The hatched area indicates the position of the tooth plates. Scale bar = 1 cm.

the jaws can open and shut in the coronal plane, and the upper jaw can rotate in the coronal plane relative to the lower jaw (Fig. 2). However, there is little relative dorsoventral translation or rotation about the long axis of the jaws. One ligament, the inner quadratomandibular ligament (IQL), joins the medial surfaces of the articular processes of the palatoquadrate and Meckel's cartilage and extends into the articular space of the jaw joint. The IQL limits the gape, prevents lateral movement of the palatoquadrate relative to Meckel's cartilage, and, to an extent, also limits relative dorsoventral movement. The other ligament, the palatoquadrate-mandibular connective tissue sheath (PML), covers the lateral aspect of the jaw joint. The PML limits rotation of the jaw elements about their long axis and dorsoventral motion of the upper and lower jaw relative to one another. In a 56-cm DW female *Rhinoptera bonasus* the maximum gape was slightly less than 20 mm, as a block of that size would not fit between the jaws for an open mouth radiograph. The ligaments of the hyomandibular-jaw articulation also serve to stabilize the joint. Though strong and dense, the ligaments are not calcified, as is evident in the CAT scan of the jaws (Fig. 3). The CAT scan reveals that jaws themselves do not articulate tightly with each other or the hyomandibula; instead, a network of soft connective tissue stabilizes the jaw. F3

While movements of the jaws are restricted relative to one another, as a unit the jaws are highly mobile. From manipulation of fresh specimens, it is clear that the shallow angle of the hyomandibulae and the lack of connective tissue connection between the upper jaw and the chondrocranium allow an impressive amount of jaw protrusion. The jaws of an adult eagle ray protruded over 60 mm, and those of an adult cownose protruded over 30 mm. Some freedom for lateral motion of the jaws was noted in both species. This protrusion presumably allows the ray to grab buried invertebrates and increases the volume of the oropharyngeal cavity during prey processing.

The teeth of the myliobatid hard prey specialists are thick, flattened, usually hexagonal units that interlock to form a band of teeth running the width of the mouth. These bands, or tooth rows, form a continuous tooth plate (Fig. 4). The youngest teeth appear as lightly calcified elements underneath a thin ligamentous sheath that covers the odontogenic tissue. The teeth are embedded in an elastin-rich dental ligament that transports them towards the occlusal plane, where they become functional. After an unknown length of time, all the teeth in a row pass aborally out of the occlusal plane and are lost (Fig. 5). As the teeth move towards the occlusal plane, they mineralize, becoming mature by the time they emerge from under the ligamentous sheath. There are three to ten rows of mature, unworn teeth behind the functional rows. The functional rows of teeth are distinguished in all the hard prey specialists by a pattern of scratches, gouges, and deep scouring that occurs where the prey is crushed and ground to pieces (Fig. 4). This wearing surface is usually two or three rows wide. The lower jaw of *Aetobatus narinari* has an exceptionally wide area of wear, in one case involving 14 rows of teeth. This unusual situation reflects a peculiarity of eagle ray anatomy. The lower jaw of *A. narinari* supports the tooth plate well beyond the area of contact with the upper jaw. After the lower jaw teeth move out of the crushing zone, they remain attached to the tooth plate and form a spade-like appendage to the lower jaw (Fig. 3). This appendage has been hypothesized to assist the animal in digging out prey items from the substrate (Gudger, 1914). F4 F5

Many bony fishes sequester iron in their teeth, presumably to strengthen them (Motta, 1987); however, the electron microprobe of *Aetobatus narinari* teeth did not reveal significant percentages of iron, manganese, or magnesium.

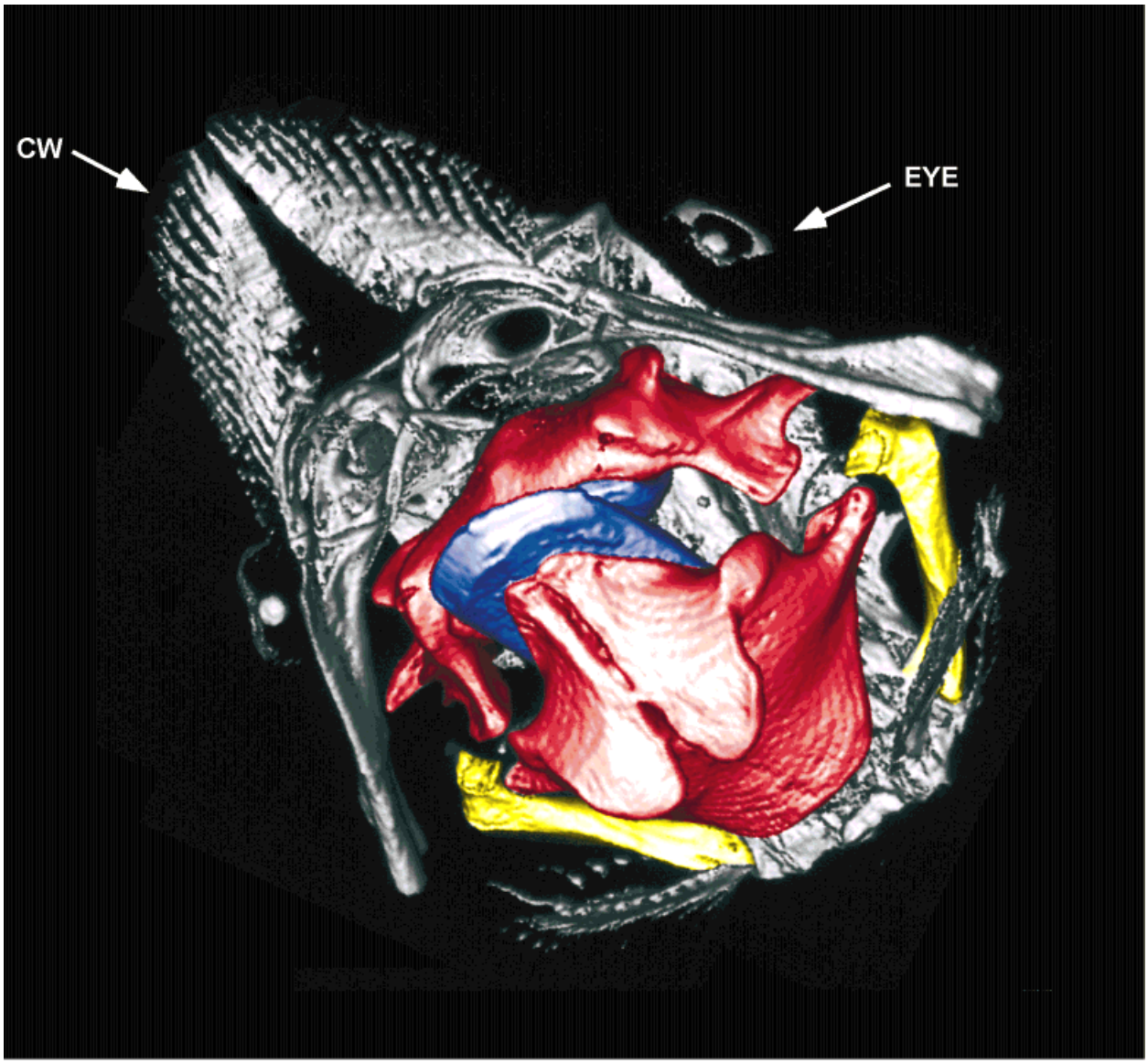

Fig. 3. Computed axial tomography scan of the head of an adult spotted eagle ray, *Aetobatus narinari*, in ventrolateral view. The tooth plates have been colored in blue, the jaws in red, and the hyomandibulae in yellow. The lower tooth plate extends beyond the area of contact with the upper tooth plate. The upper left corner (anterior) of the scan shows the cephalic-wing fin rays (CW) characteristic of the myliobatids. Both eyes with their lens show in the image, with the left eye and its lens in the upper right corner.

Calcified Cartilage

The prismatic cartilages of the jaws exhibit analogs to cortical thickening and trabeculation, the two ways that bone is strengthened. The cartilaginous analog to cortical thickening, multiple layers of tesserae, is visible in the histological and radiographic sections of the jaws of *Dasyatis sabina, Rhinoptera bonasus, Myliobatis californicus* and *Aetobatus narinari.* The entire surface of the jaws of *R. bonasus* is covered by at least two layers of tesserae and in areas there are as many as six layers. These very thick areas are at the center of the jaws on the surface opposite the crushing tooth plates (Fig. 5).

Examination of other species revealed that multiple layers of tesserae are a widespread phenomenon. The "saw" of the sawfish, *Pristis pectinatus*, is well reinforced with multiple layers of tesserae. There are three or four layers in the outer surface of the "saw" and six or more in the wall that runs internally along its length. Dried skeletal tissue of *Isurus oxyrhynchus* and *Hydrolagus colliei* has more than one layer of tesserae in the jaws, though it is difficult in dried tissue to distinguish whether this is an artifact of shrinkage.

Trabeculation, the other mechanism by which bone is strengthened, was found in the jaws of all of

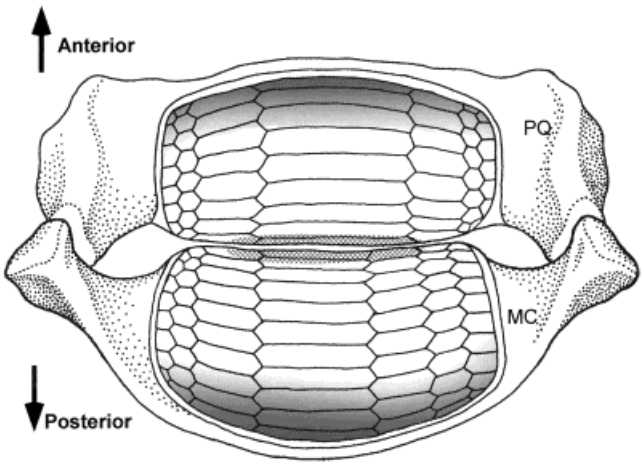

Fig. 4. Drawing of the upper and lower jaws of the cownose ray, *Rhinoptera bonasus*, in their correct anatomical position. The mouth of stingrays is ventrally directed rather than the more familiar terminal mouth of other fishes. This illustrates a dorsal view of the jaws seen from inside the mouth looking down. The teeth are formed at the posterodorsal margin of Meckel's cartilage and the anterodorsal margin of the palatoquadrate. The tooth plates are not well mineralized when they are first formed (indicated as darker teeth) but are fully mineralized when they emerge from under a thin tendinous sheet covering the odontogenic tissue. The hatched area, showing tooth wear, is very small relative to the surface area of exposed, fully mineralized teeth.

the durophagous stingrays examined. Radiographs of *Rhinoptera bonasus* do not clearly show the trabecular cartilage (Fig. 2) unless the tooth plates are first removed (Fig. 5). In radiographs with the tooth plates removed, a network of trabeculae (struts) is visible, as are the hollow ends of the trabeculae. Radiographs of a series of sagittal sections show the extensive nature of the trabeculation. The shape of the jaw in cross section is variable, but there are trabeculae in every section, from the center of the jaws to the lateral-most corner. The struts are oriented in such a way as to transfer the crushing forces to the multiple layers of prismatic cartilage opposite the tooth plates.

Histological sections of the jaws show the trabeculae to be hollow structures, walled with blocks of calcified material that appears identical to the tesserae of the prismatic surface layer. In thin sections, the trabeculae are cut obliquely and appear as unstained ovals surrounded by tesserae and hyaline cartilage (Fig. 6b). The central lumen of a strut contains no cellular material and is not lined with epithelial tissue. In the cownose ray jaws, there was no evidence that the hollow struts pierced the surface of the jaw. The tesserae of the struts simply become indistinguishable from the tesserae of the surface and, presumably, some tesserae cover the open end of the lumen, where it contacts the surface. The jaws of an eagle ray (*Aetobatus narinari*) showed a different morphology. Some struts end in open holes in the surface of the jaws. The number of open-ended struts appeared to be far fewer than the number of struts that showed on radiographs, indicating that not every strut is open-ended.

Tesserae, the calcified blocks that cover the surface of the jaws and the walls of the trabeculae, have a higher density of smaller cell spaces than the surrounding hyaline cartilage matrix. Tesserae that make up the trabeculae are surrounded on all sides by hyaline cartilage (Fig. 6c,d). Even the surface of a tessera that faces the lumen of the strut has a thin, cellular layer of uncalcified cartilage. In places, the cartilage lining the lumen appears to be made up of several layers (Fig. 6e). Polarized light microscopy reveals that a layer of collagen fibers surrounds the tesserae. This layer sends Sharpey's fibers into the mineralized cartilage. Tesserae in the walls of the struts are often, though not always, linked by collagen fibers. Occasionally, isolated tesserae or pairs of tesserae are found within the central region of uncalcified hyaline cartilage matrix (Fig. 6f).

Ontogeny

An ontogenetic series of *Rhinoptera bonasus* demonstrates that the struts form before birth. Adult fish were all eating hard prey, as evidenced by extensive wear to the tooth plates and shells in the intestine. A prominent umbilical scar on the smallest juvenile, a 32-cm DW male specimen, showed that it was a recent birth. Examination of the gut contents found the intestine full of crushed shells, just as in the adult fishes. Tooth plates already had extensively worn surfaces, and the radiographs showed trabeculation similar to that of the adult (Fig. 7). A single, late-stage embryo, 21 cm DW, had an empty stomach and no wear marks on the teeth at all. Even when examined at 50× magnification with a dissecting microscope there was no evidence that the tooth plates had been ground together in utero. Radiographs of sagittal sections showed the trabeculation to be of the same form as in the adult and juvenile animals (Fig. 7).

There was no indication, in any sections, of partially formed struts. Partially formed struts might either start in the center of the jaw and not reach the outer surface, or start at the surface and not grow all the way through. The struts appear to grow in diameter with increasing size of the animal; however, an exact figure for the growth could not be measured because of the overlapping struts in each radiograph. The sawn sections were the same thickness for the different sizes of animals. In smaller animals there were more struts overlying one another in each section, which made it difficult to measure widths of trabeculae in smaller animals.

Phylogenetic Distribution

The comparative material examined for the presence of trabecular cartilage included most of the genera in the Myliobatidae and six genera of batoids

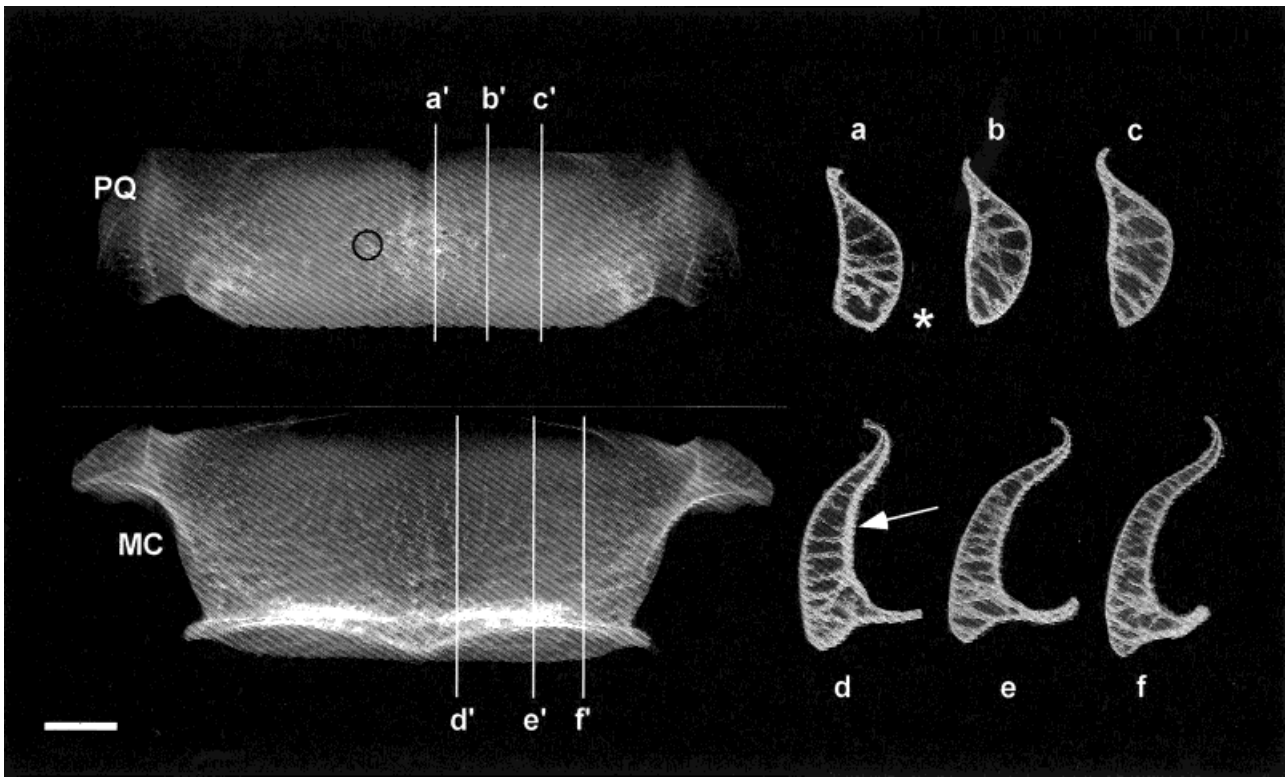

Fig. 5. A composite radiograph of the palatoquadrate (PQ) and Meckel's cartilage (MC) from an adult cownose ray, *Rhinoptera bonasus*. The left radiograph shows the jaws after the tooth plates have been stripped away. The lower jaw (MC) is shown in an anteroposterior view with ventral towards the bottom of the figure. The crushing area of the tooth plates would have been around the brightest white area near the bottom of the figure. The upper jaw (PQ) is shown in dorsoventral view, with anterior at the bottom. The crushing area of the tooth plates would have been along the bottom edge of the radiograph. Parasagittal sections (1–3 mm thick) taken from these jaws are shown on the right, and for all sections anterior is on the left and dorsal is at the top. Each section was taken in approximately the plane indicated by the corresponding section line. There is considerable variation in the shape of the cross section from medial to lateral; however, struts are evident in all sections. The tooth-bearing surfaces of the sections are shown schematically on one section from each jaw, with the darkest teeth being least calcified and the lightest most calcified. The area of high tooth wear is indicated by an asterisk. Hollow trabeculae can be seen end-on in some areas of the whole jaw radiographs, as indicated by the black circle. The arrow on section (d) indicates an area of particularly thick prismatic cartilage on the nontooth-bearing surface of a section of the lower jaw. Scale bar = 1 cm.

F8 outside the family (Fig. 8). All of the myliobatid stingrays in this study, *Myliobatis californica, Rhinoptera bonasus, Aetobatus narinari,* and the planktivorous *Manta birostris* had trabecular cartilage in their jaws. The three hard prey specialists showed no qualitative difference in the pattern of struts in the trabecular cartilage. The wedge-shaped piece of jaw removed from a manta ray (*M. birostris*) jaw had trabeculae of a similar diameter to the other myliobatids. However, the pattern of trabeculation could not be determined because the mouth of the animal examined for this study is over 100 cm wide, and transporting the head to the radiographic facility was not practical. The only other material available was an embryonic manta that radiographed poorly, either because the embryo was poorly mineralized or because formalin fixation dissolved the existing mineral.

Examination of the sister taxon to the Myliobatidae, the butterfly ray *Gymnura altivela*, revealed no trabecular cartilage. Trabecular cartilage was also absent from the other three stingray taxa sampled, *Dasyatis sabina, Urolophus jamaicensis* and *Taeniura lymma*. The sister taxon to the stingrays (Myliobatiformes) contains both the skates (Rajidae) and a genus of guitarfish (*Rhinobatos*). Individuals from these two taxa, *Rhinobatos lentiginosus*, *Leucoraja erinacea*, and *Raja ocellata,* exhibited no trace of trabecular cartilage in their jaws.

Model of Jaw Function

The anatomy of the jaws of hard prey specialists suggests that the combination of gape-limiting ligaments (IQL and PML) and a well-fused mental symphysis will multiply the force of the adductor muscles during crushing. The upper and lower jaw are modeled as rigid bars with inextensible ligaments that link the lateral margins of the jaw together. Crushing a prey item requires the jaws to open some distance, which takes up some of the slack in the ligaments at the jaw joint. Assuming that the jaw

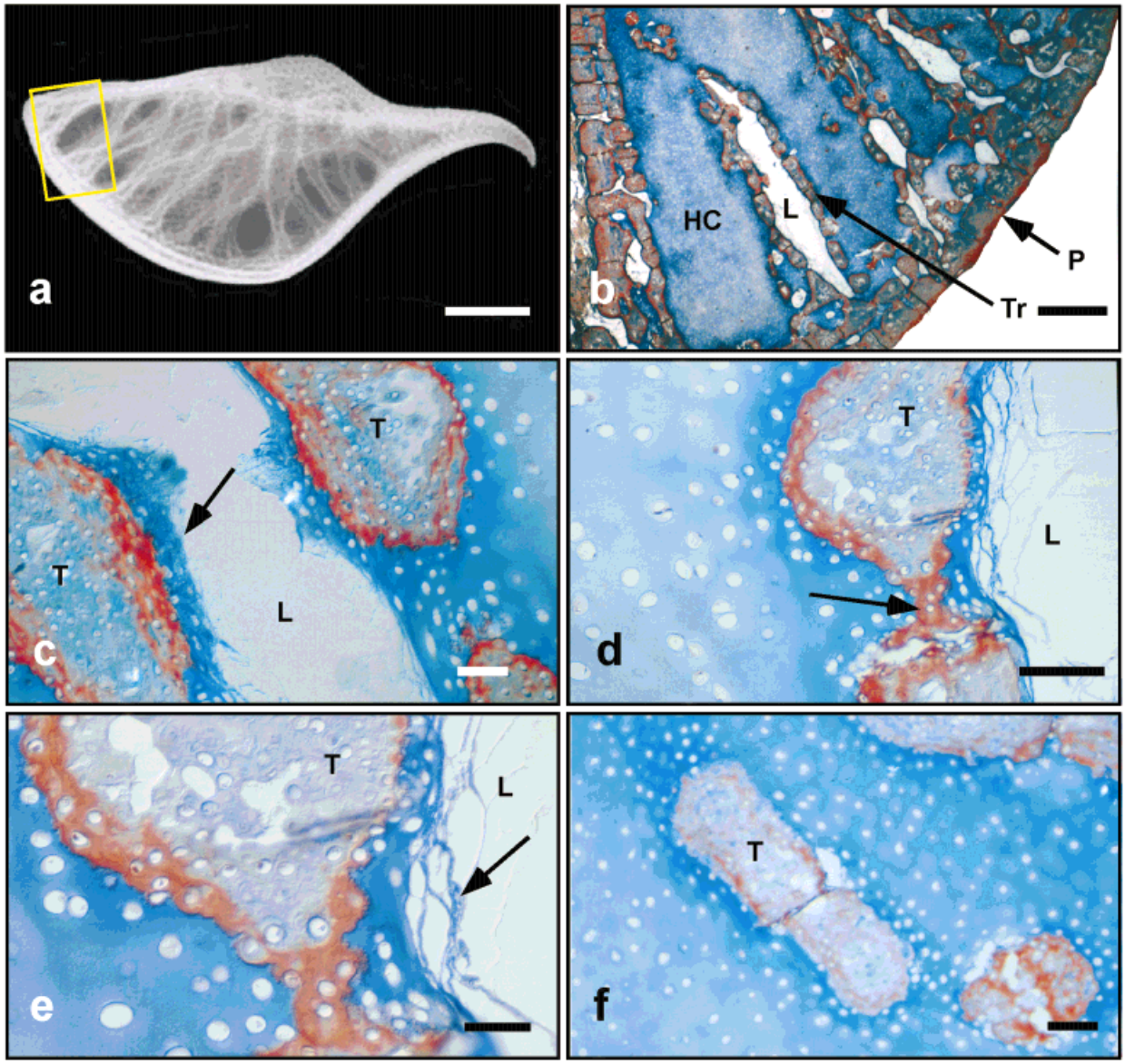

Fig. 6. Histological sections, in the parasagittal plane, from the palatoquadrate of a cownose ray, *Rhinoptera bonasus*. **a**: A radiograph of a section of the upper jaw. The yellow box indicates from where the sections in the remaining figures (**b–f**) are taken. Scale bar = 7 mm. The remaining sections (**b–f**) were stained with Masson's trichrome and photographed with differential interference contrast lighting. **b**: A section of the jaw showing normal hyaline cartilage (HC) surrounded by an outer layer of prismatic cartilage (P) and containing several trabeculae (Tr). The hollow trabeculae are cut slightly obliquely so that each is represented by an oval of tesserae surrounding an unstained lumen (L). Scale bar = 700 μm (modified from Summers et al., 1998). **c**: The tesserae (Te) surrounding the lumen (L) of the trabeculae are themselves surrounded by hyaline cartilage. A thin layer of basophilic tissue lines the lumen (arrow). Scale bar = 30 μm. **d**: Many tesserae appear joined by collagen fibers. Cells are smaller and denser within the tesserae than they are in the surrounding matrix. Scale bar = 30 μm. **e**: In some areas, thin sheets of basophilic matrix loosely line the lumen of the trabeculae (arrow). Scale bar = 10 μm. **f**: A pair of tesserae surrounded by matrix. These unassociated calcified blocks are not common, but demonstrate that the lumen is not needed for calcification of tissue. Scale bar = 30 μm.

adductors contract unilaterally, as they do in some other batoids (Summers, 1995), the upper jaw would rotate relative to the lower jaw, taking up the remaining slack in the ligaments on one side. The jaws now act as a second order lever system, with the adductor on one side providing an input force, the ligaments on the other side forming the fulcrum, and the prey item between them receiving the output force. The familiar steel nutcracker is a good analogy for this model of jaw function, with the handles being the upper and lower jaw and the hinge being the IQL and PQL (Fig. 9). F9

The in-lever (L_{in}) is the distance between the line of action of the adductor and the ligament on the opposite side. The out-lever (L_{out}) is the distance between the prey item and the ligament (Fig. 9). The

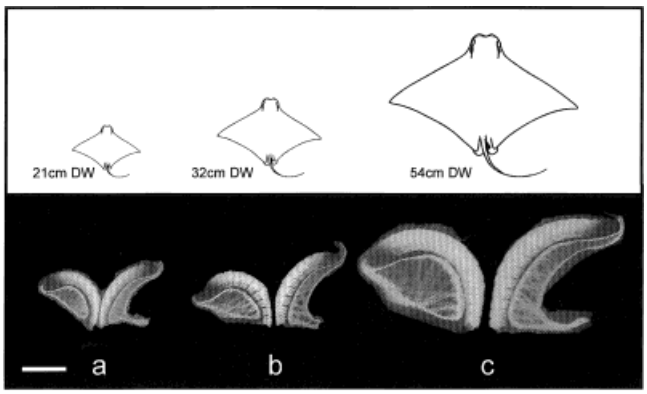

Fig. 7. An ontogenetic series of parasagittal sections, ~1–2 mm thick, from the jaws of the cownose ray, *Rhinoptera bonasus*. The three sets of sections correspond to (a) a late stage embryo, (b) a neonate, and (c) an adult. The relative sizes of the individuals are shown in the scale drawings above each pair of jaws. The palatoquadrate is on the left and Meckel's cartilage is on the right in each pair. Jaws and tooth plates were sectioned in situ, so these radiographs accurately represent the anatomical relationship of these elements. Wear patterns on the teeth are evident in the adult and in the neonate. The calcification pattern of the teeth is shown by the newly formed teeth at the upper part of each radiograph being less radio-opaque.

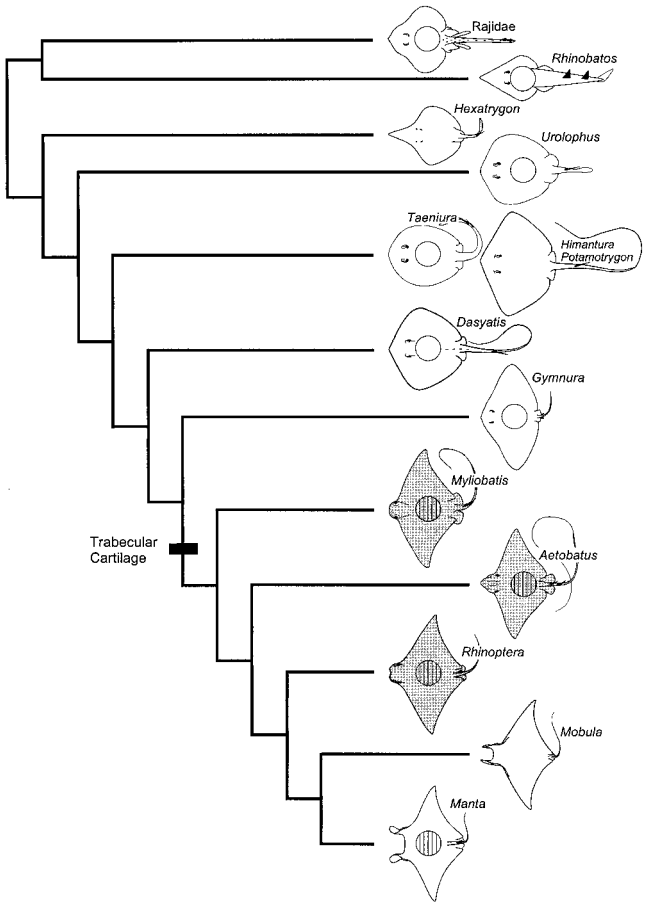

Fig. 8. Simplified cladogram of stingrays (Myliobatiformes) including two outgroups, the skates (Rajidae) and the guitarfish (*Rhinobatos*) (tree from McEachran et al., 1996, with some taxa omitted for clarity). Presence/absence of trabecular cartilage was assessed in a single species for each genus. Hard-prey specialists in the Myliobatidae are indicated with shading. Hatched circles indicate the presence of trabecular cartilage, and open circles indicate that no trabecular cartilage was found in the jaws. Unsampled taxa have no circle. Trabecular cartilage evolved once at the base of the myliobatid clade.

force at the prey item (F_{out}) is determined by the force of contraction of the adductor (F_{in}) and the relative lengths of the in and out levers (L_{in} and L_{out}) in the following way: $F_{out} = F_{in}*(L_{in}/L_{out})$ (Withers, 1992). If the prey item is exactly in the center, the force of the jaw adductor is doubled, as $L_{in}/L_{out} = 2$. In this case, although only one adductor contracts the force is equivalent to both adductors contracting at the same time. A doubling of the applied force is the minimum expected for any given location of the prey item. As the location of the prey item shifts closer to one adductor, thereby lessening that force multiplier, it moves further from the other, yielding an increase in the multiplier for that muscle (Fig. 10). The wear patterns on the teeth of the cownose ray indicate that most prey is crushed within a quarter jaw width of the center of the jaws. This indicates a 2–4-fold multiplication of the adductor force.

F10

DISCUSSION

"Crushing clams with cartilaginous jaws is like trying to fell a tree with a sock full of custard." — Henry Gee

Crushing Hard Prey

Durophagous stingrays circumvent the constraint imposed by their cartilaginous skeleton with a suite of morphological innovations. These include pavement-like dentition, a fused mandibular symphysis, strong ligaments between the jaws, prismatic cartilage, multiple layers of tesserae, and trabecular cartilage. The dentition is set in an elastic ligament that may absorb energy as the tooth plates flex relative to one another during crushing. The fused mandibular and palatoquadrate symphyses, and the reduced mobility of the upper and lower jaw relative to each other, combine to amplify the force of the jaw adductors. Lastly, the cartilage itself is strengthened in two ways, both by thickening of the outer mineralized layer and by the deposition of mineralized struts within the core of both the upper and lower jaws.

The proposed "nutcracker" model of jaw function is a rare example of a muscle acting at a large force advantage. In a lever system, a force advantage occurs when the input lever arm is longer than the output lever arm. The three classes of levers are defined by the relative positions of the fulcrum, the input force and the output force (Withers, 1992). In a class 2 lever system, the fulcrum is a fixed point at the far end of the lever and the output force is

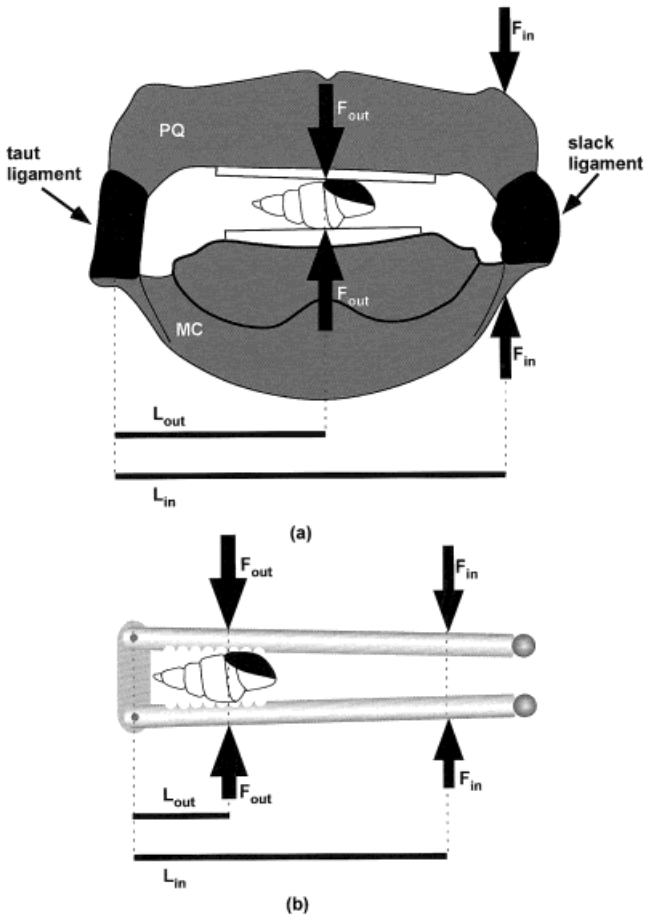

Fig. 9. **a**: The "nutcracker" model of the force advantage of the jaws of the cownose ray, *Rhinoptera bonasus,* in ventral view. A gastropod is shown between the tooth plates, acted upon by a second-class lever powered by the adductors. The ligaments between the upper and lower jaws, shown in black, serve as the fulcrum of the lever system. **b**: A nutcracker of similar proportions showing the principles of the second-order lever system.

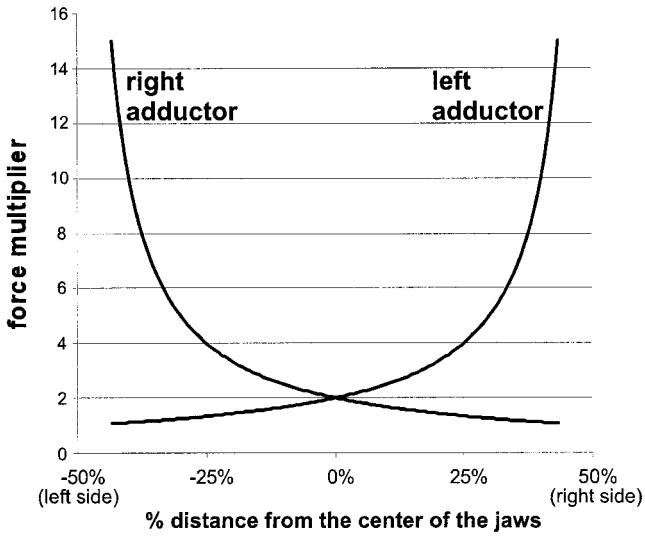

Fig. 10. Graph of the force advantage of the adductor muscles vs. prey position. The x-axis shows the position of the prey item relative to the center of the jaw. The y-axis shows the force advantage of the left and the right adductor muscle, contracting singly, computed as the ratio of the length of the in lever to the out lever.

measured between the fulcrum and input force. Class 2 levers multiply the input force at the expense of velocity because the input lever is always greater in length than the output lever. Another example of a class 2 lever is the human foot lifting onto its toes. The ball of the foot acts as the fulcrum, while the foot extensors in the lower leg generate an input force acting at the distal end of the heel bone (calcaneus). The output force is exerted on the lower leg at the tibiotarsal joint, which is between the calcaneus and the ball of the foot. The input lever is the distance from the end of the calcaneus to the ball of the foot and the output lever is from the ball of the foot to the tibiotarsal joint.

The nutcracker model could be tested in several ways. The most direct method requires measuring force production in live animals, with simultaneous confirmation that the jaw adductors are firing asynchronously. The difficulties of this are the usual ones associated with eliciting a natural behavior, such as feeding under experimental conditions (Liem, 1976; Motta et al., 1991). An alternative to measuring force production directly would be to infer maximum force production from the force required to crush known hard prey items. This estimate of force could then be compared to the theoretical maximum, given the cross-sectional area of the adductor muscles (Wainwright, 1988; Hernandez and Motta, 1997). There is a body of dietary data on the hard prey specialists, including a spectacular report that an eagle ray crushed a clam that ". . .weighed more than three pounds, and to crack which perhaps a pressure of 1000 pounds would be required" (Coles, 1910, p. 339). This literature notwithstanding, the complex architecture of the adductors, including at least six separate slips of muscle (Miyake, 1988), would make the computation of effective cross-sectional area difficult.

Three structural and functional characteristics of the jaw system are required for the nutcracker mechanism to work: 1) fused mandibular and palatoquadrate symphyses, 2) palatoquadrate-mandibular ligaments limiting gape, and 3) jaw adductors firing asynchronously. These factors make it unlikely that the other two cartilaginous hard prey specialists, chimaeras and horn sharks, use this method of force amplification. Although horn sharks, *Heterodontus sp.*, have pavement-like dentition, they lack well-fused symphyses in the upper and lower jaw (Garman, 1913; Smith, 1942). Additionally, several studies of jaw muscle activity in sharks have not indicated any asynchronous activity (Motta et al., 1991, 1997; Wilga and Motta, 1998). In holocephalans, or chimaeras, tooth plates and a well-fused mandibular symphysis are

present, and the palatoquadrate is completely fused to the chondrocranium. However, these fish are so laterally compressed that the input and output levers would be very short, and there does not appear to be a strong, gape-limiting ligament between the lower jaws and the chondrocranium (Garman, 1904; Grogan et al., 1999).

Calcified Cartilage

Several configurations of tesserate prismatic cartilage—including multiple layers of tesserae, endochondral tesserate struts (trabecular cartilage), and tesserae isolated in the hyaline ECM—were found in the jaws of the durophageous stingrays. Prismatic calcification, the material of the tesserae, has been described as being in close association with the fibrous perichondral layer (Kemp and Westrin, 1979; Clement, 1992). Since the perichondral surface is vascular, molecular signals in the blood might directly trigger mineralization of the hyaline cartilage. Alternatively, signals could be generated by the fibroblasts of the perichondrium. In either case, chondrocytes near the surface initiate mineralization and continue the process as the mineralizing wave invades the hyaline cartilage core. However, there is no plausible explanation for the deposition of a block of mineralization within the avascular hyaline core. This has made the few reports of subperichondral tesserae problematic from a developmental point of view (Schaeffer, 1981; Dingerkus et al., 1991).

This study found that multiple layers of tesserae, in which only the outer layer is in contact with the perichondrium, are a plesiomorphy of the cartilaginous fishes, based on their occurrence in every taxon examined. There are several possible explanations for this subperichondral mineralization. The multiple layers are found in places where loads, and local strains, are presumed to be high. Tesserae of the subperichondral layers could have mineralized at the perichondral surface, and then been forced under adjacent tesserae by the strains imposed by high loads. Alternatively, the layers could represent separate developmental waves of tesserae formation, where the perichondrium has induced formation of new tesserae on top of mature tesserae. There is some evidence from chick embryos of multiple waves of cartilage deposition in a mineralizing field (Fang and Hall, 1995). This latter explanation is considered more probable because of the continuous, intact nature of the inner layers of tesserae.

Trabecular cartilage is less easily explained as mineralization originating from the perichondrium. The open-ended struts found in the eagle ray may develop as invaginations of the perichondrium, but there is no indication of fibrous perichondrium lining the trabeculae of the cownose ray. These struts, and the closed-ended struts of the eagle ray, must have another route to mineralization. One possible developmental scenario is that the trabeculae grow in length by adding tesserae to the ends of the columns, and increase in complexity by branching at the surface and then increasing in length as the jaws grow. Mineralizing tesserae would always be at the surface, with already mineralized blocks becoming internal as the jaws grow larger. The observation that the struts increase in diameter during ontogeny may be at odds with this developmental pattern. This scenario would not account for struts that become wider throughout their length. The radiographs did not clearly show whether the struts in the larger animals had a thin central region or a constant diameter.

Cartilage canals are epithelial-lined tunnels that carry nerves and blood vessels through hyaline cartilage. Cartilage canals have been described from most vertebrates (Kuettner and Pauli, 1983), including elasmobranchs (Leydig, 1857). It is possible that trabeculae are a calcified, degenerate-form canal, lacking the vessels, nerves, and lining. Biochemical signals, or connective tissue stem cells, could move through the interstitial fluid and down these canals, thus inducing mineralization of the walls. Although we do not understand the process by which the vascularized mesenchyme of a cartilage canal invades hyaline cartilage, it appears to be a common phenomenon in cartilaginous elements greater than 3 mm in diameter (Moss and Moss-Salentijn, 1983). If trabeculae are degenerate, mineralized cartilage canals, then they may well increase in diameter over their entire length during ontogeny. Tesserae would then be added to the outer walls of the canal in the same way they are added to the outer surface as the skeletal element grows.

The thin layer of unmineralized cartilage on the luminal surface of the tesserae in the walls of the struts may be important in explaining tesserae found deep within the hyaline cartilage core of a skeletal element (Kemp and Westrin, 1979). Under some circumstances, in a localized region, the cells of the unmineralized tissue between the lumen of the strut and the tesserae could proliferate and make more extracellular matrix. This would result in one or several tesserae surrounded on all sides by hyaline cartilage.

The formation of trabecular cartilage could be in response to mechanical loading or it could be a genetically determined pattern of mineralization. Two lines of evidence suggest that trabeculae are not induced by mechanical loading: 1) the presence of trabeculae in young rays prior to feeding, and 2) the trabecular cartilage of the manta ray. Since both the newly born and the embryo cownose ray had well-developed trabeculae, the stress of eating hard prey can be ruled out as the epigenetic cue for strut formation. This does not, however, rule out the possibility that the struts are an epigenetic effect. Muscle activity during embryogenesis has profound effects on the structure on the skeletal system

(Herring, 1990), including mineralization of cartilage (Fang and Hall, 1995). Perhaps contractions of the jaw adductors during early embryonic development are instrumental in patterning the mineralization of the trabeculae.

The retention of trabecular cartilage by the planktivorous manta ray also has bearing on the question of whether trabecular cartilage has a genetic basis. The presence of struts in an animal that does not eat hard prey is evidence that trabeculae are genetically determined. However, trabecular cartilage may not be as useless to the manta ray as it may at first appear. Mantas are particularly large stingrays, at 6 meters in width and over 1,500 kg (Bigelow and Schroeder, 1953). Moreover, their large terminal mouth is held open against the flow of water as they suspension-feed on plankton. The wide expanse of jaw resisting the force of the water may require reinforcement to prevent failure by buckling. The answer to the question of epigenesis will be found either in manipulations of early embryos, or in culturing trabecular cartilage in vitro. The reproductive mode of the Myliobatidae makes the first approach problematic, as they give live birth to a single, large embryo each year (Bigelow and Schroeder, 1953; Schwartz, 1965; Hamlett et al., 1985).

Implications for Paleontology

Isolated teeth and tooth plates are the primary constituent of the chondrichthian fossil record (e.g., Eastman, 1903; Herman et al., 1989; Feibel, 1993). There are, however, some significant and complete endoskeletal remains (e.g., Romer, 1964; Lund, 1990; Maisey, 1993; Coates et al., 1998). The association of multiple layers of tesserae and trabecular cartilage with areas of high stress is a basis for making predictions about the functional morphology and habits of fossil taxa. For example, perhaps the multiple layers of tesserae in xenacanthines (Schaeffer, 1981) are an indication that they were durophagous, crushing prey with muscles that pulled the lower jaw against both the upper jaw and chondrocranium.

The forms of mineralized cartilage described in this study also affect the interpretation of early vertebrate fossils. Many agnathans and early gnathostomes are known only from dermal scales, although a few specimens preserve endoskeletal tissue (Long, 1995). For example, the evolutionary origin of endochondral bone is supported by calcification that appears to be within a skeletal element (Smith and Hall, 1990). Since trabecular cartilage, like endochondral bone, has strut-like internal mineralization, reexamination of this fossil, and consequently the placement of endochondral bone on the vertebrate cladogram, would be in order.

The evolution and morphology of hard tissues has been extensively addressed from a paleontological point of view (Ørvig, 1951, 1968; Halstead, 1974; Smith and Hall, 1990; Forey and Janvier, 1993; Coates et al., 1998), and extant models can be useful in understanding fossil morphology. Ørvig (1951) described three types of calcified cartilage from fossil fishes: globular, prismatic, and areolar. He hypothesized that these three may form a transition series, with globular calcification becoming either areolar or prismatic either through evolutionary time or ontogeny. Trabecular cartilage, with its multiple layers of tesserae and internal struts, may exhibit more than one type of calcification. Sections of trabecular cartilage seem to show the "Liesengang lines" that usually characterize globular calcified cartilage (Fig. 6e), rather than the prismatic cartilage associated with tesserae. This raises the question whether certain regions of the tesserae that make up the struts are prismatic while others are globular.

Liesengang lines are central to another question raised by fossil tissue. They are thought to be evidence of the progression of the mineralizing wave as it passes through the unmineralized tissue (Ørvig, 1951). The waves are affected by holes in the fossil tissue, which are thought to be cell spaces. In some instances, it appears that the lines are emanating from the putative cell spaces. From the mineralization pattern of Recent tissues it is clear that the cells should not be the centers of mineralization. Endochondral mineralization during bone formation does not take place around chondrocytes (Ali, 1983). Mineralization starts in matrix vesicles some distance from the cell lacunae. This raises two questions: 1) are the lacunae in the fossil tissue actually cell spaces; and 2) is the mineralization emanating from the cell spaces, as the Liesengang lines might suggest?

This study highlights the innovative morphology with which cartilaginous fishes solve the problem of crushing hard prey. By comparing the functional morphology of bony and cartilaginous fishes, it is possible to explore the opportunities and constraints imposed by very different skeletal materials. In this case, our understanding of cartilage as a material is expanded to include new conformations of calcification. Other functional extremes of cartilaginous fishes will yield equally interesting insights into the ways in which cartilage is used as a primary structural element, rather than as an adjunct to bone.

ACKNOWLEDGMENTS

This study would not have been possible without the generous logistical and intellectual assistance of several people and organizations. The Shriners Hospital for Children in Tampa, FL, allowed me to use their X-ray and histology facility. Walter McAllister was a vital histological resource. Donna King and Paul Kolbjornsen at Cooley-Dickinson Hospital made the images used for the 3-D reconstructions. Charlie Manire at Mote Marine Lab in Sarasota, FL, captured most of the animals in this study. Gary

Nelson at the DEP in St. Petersburg supplied several animals, and Lisa Rosenberger at the University of Chicago rushed me an important specimen on short notice. J.D. Dubbick of the University of Puerto Rico kindly sent me the series of spotted eagle rays. Karsten Hartel and the collections staff at the Museum of Comparative Zoology helped me find and radiograph material and provided stimulating lunch discussions. This manuscript has benefited from style and content suggestions from Beth Brainerd, Brian Hall, Rachel Simons, Jim O'Reilly, Alex Patton, Lara Ferry-Graham, and Moya Smith. Dr. Frederick Harrison very kindly edited an earlier draft of the manuscript. John Maisey has been a helpful idea bank. The weekly meetings of the comparative physiology lab group at the University of Massachusetts influenced the ideas and structure of the article.

LITERATURE CITED

Ali SY. 1983. Calcification of cartilage. In: Hall BK, editor. Cartilage. New York: Academic Press. p 343–378.

Bigelow HB, Schroeder WC. 1953. Sawfishes, guitarfishes, skates and rays. In: Tee-Van J, editor. Fishes of the western North Atlantic. New Haven: Sears Foundation for Marine Research. p 1–514.

Biknevicius AR. 1996. Functional discrimination in the masticatory apparatus of juvenile and adult cougars (*Puma concolor*) and spotted hyenas (*Crocuta crocuta*). Can J Zool 74:1934–1942.

Clement JG. 1986. Development, structure and composition of chondrichthyan skeletal tissues. PhD Thesis. London: University of London.

Clement JG. 1992. Re-examination of fine structure of endoskeletal mineralization in chondrichthians: implications for growth, aging and calcium homeostasis. Aust J Mar Fresh Res 43:157–181.

Coates MI, Sequeira SEK, Sansom IJ, Smith MM. 1998. Spines and tissues of ancient sharks. Nature 396:729–730.

Coles RJ. 1910. Observations on the habits and distribution of certain fishes taken on the coast of North Carolina. Bull Am Mus Nat Hist 28:338–341.

Compagno LJV. 1984. Sharks of the world — an annotated and illustrated catalogue of shark species known to date. New York: United Nations FAO Guide.

Dean B. 1906. Chimaeroid fishes and their development. Washington: Carnegie Institution.

Dingerkus G, Seret B, Guilbert E. 1991. Multiple prismatic calcium phosphate layers in the jaws of present-day sharks (Chondrichthyes; Selachii). Experientia 47:38–40.

Eastman CR. 1903. Reports on the scientific results of the expedition to the tropical Pacific, in charge of Alexander Agassiz, in the U.S. Fish Commission steamer "Albatross," from August, 1899 to March, 1900, Commander Jefferson F. Moser, U.S.N., commanding. Part V. Sharks teeth and cetacean bones from the red clay of the tropical Pacific. Mem Mus Comp Zool 26:179–189.

Fang JM, Hall BK. 1995. Differential expression of neural cell adhesion molecule (NCAM) during osteogenesis and secondary chondrogenesis in the embryonic chick. Int J Dev Biol 39:519–528.

Feibel CS. 1993. Freshwater stingrays from the plio-pleistocene of the Turkana basin, Kenya and Ethiopia. Lethaia 26:359–366.

Forey P, Janvier P. 1993. Agnathans and the origin of jawed vertebrates. Nature 361:129–134.

Gans C. 1952. The functional morphology of the egg eating adaptations in the snake genus *Dasypeltis*. Zoologica 37:209–244.

Garman S. 1904. The chimeroids (Chismopnea Raf, 1815; Holocephala Mull., 1834), especially *Rhinochimera* and its allies. Bull Mus Comp Zool 41:243–272.

Garman S. 1913. The Plagiostomia. Mem Mus Comp Zool 36:1–515.

Gosner KL. 1993. Scopate tomia, an adaptation for handling hard-shelled prey? Wilson Bull 105:316–324.

Grogan ED, Lund R, Didier D. 1999. Description of the chimaerid jaw and its phylogenetic origins. J Morphol 239:45–59.

Gudger EW. 1914. History of the spotted eagle ray, *Aëtobatus narinari,* together with a study of its external structures. Carnegie Institution of Washington 183:241–323.

Gudger EW. 1915. The natural history of the whale shark *Rhineodon typus* Smith. Zoologica 1:349–387.

Halstead LB. 1974. Vertebrate hard tissues. London: Wykeham Publications.

Hamlett WC, Wourms JP, Smith JW. 1985. Stingray placental analogues: structure of trophonemata in *Rhinoptera bonasus*. J Submicrosc Cytol 17:541–550.

Herman J, Hovestadt-Euler M, Hovestadt DC. 1989. Contributions to the study of the comparative morphology of teeth and other relevant ichthyodurulites in living supraspecific taxa of chondrichthian fishes. A: Selachii. No 3: order squaliformes families: echinorhinidae, oxynotidae, and squalidae. Bull Inst R Sci Nat Belg 59:101–157.

Hernandez LP, Motta PJ. 1997. Trophic consequences of differential performance: ontogeny of oral jaw-crushing performance in the sheepshead, *Archosargus probatocephalus* (Teleostei, Sparidae). J Zool 243:737–756.

Herrel A, Wauters I, Aerts P, De Vree F. 1997. The mechanics of ovophagy in the beaded lizard, *Heloderma horridum*. J Herpetol 31:383–393.

Herring S. 1990. Development of functional interactions between skeletal and muscular systems. In: Hall BK, editor. Bone — differentiation and morphogenesis of bone. Ann Arbor, MI: CRC Press.

Homberger DG. 1988. Filing ridges and transversal step of the maxillary rhamphotheca in Australian cockatoos (Psittaciformes: Cacatuidae): a homoplasic structural character evolved in adaptation to seed shelling. In: van den Elzen R, Schuchmann K, and Schmidt-Koenig K, editors. Current Topics in Avian Biology. Stuttgart: Ver Deutsch Ornith Ges.

Homberger DG, Brush AH. 1986. Functional morphological and biochemical correlations of the keratinized structures in the African grey parrot, *Psittacus erithacus* (Aves). Zoomorphology 106:103–114.

Humason GL. 1972. Animal tissue techniques. San Francisco: W.H. Freeman.

Kemp NE, Westrin SK. 1979. Ultrastructure of calcified cartilage in the endoskeletal tissue of sharks. J Morphol 160:75–102.

Kuettner KE, Pauli BU. 1983. Vascularity of cartilage. In: Hall BK, editor. Cartilage. New York: Academic Press. p 281–308.

Lappin AK. 1997. Feeding ecomorphology of crotaphytid lizards: using bite force performance to link morphology to behaviour. J Morphol 232:284.

Last PR, Stevens JD. 1994. Sharks and rays of Australia. Melbourne, Australia: CSIRO.

Leydig F. 1857. Lehrbuch der Histologie des Menschen und der Tiere. Frankfurt: Meidinger.

Liem KF. 1976. Evolution of the scale-eating cichlid fishes of Lake Tanganyika: a generic revision with a description of a new species. Bull Mus Comp Zool 147:319–350.

Long JA. 1995. The rise of fishes: 500 million years of evolution. Baltimore: Johns Hopkins University Press.

Lovejoy NR. 1996. Systematics of myliobatid elasmobranchs: with emphasis on the phylogeny and historical biogeography of neotropical freshwater stingrays. Zool J Linn Soc 117:207–257.

Lund R. 1990. Chondrichthyian life history styles as revealed by the 320 million years old Mississippian of Montana. Env Biol Fishes 27:1–19.

Maisey JG. 1993. The interrelationships of protospinax elasmobranchii hypnosqualea reviewed in the light of new material. J Vert Paleontol 13:48A.

McEachran JD, Dunn KA, Miyake T. 1996. Interrelationships of batoid fishes (Chondrichthyes: Batoidea). In: Stiassny MLJ, Parenti LR, Johnson GD, editors. Interrelationships of fishes. New York: Academic Press. p 63–84.

Miyake T. 1988. The systematics of the stingray genus *Urotrygon* with comments on the relationships within Urolophidae (Chondrichthyes, Myliobatiformes). PhD Dissertation. College Station, Texas: Texas A&M University.

Moss ML. 1977. Skeletal tissue in sharks. Am Zool 17:335–342.

Moss ML, Moss-Salentijn L. 1983. Vertebrate cartilages. In: Hall BK, editor. Cartilage. New York: Academic Press. p 1–24.

Motta PJ. 1987. A quantitative analysis of ferric iron in butterflyfish teeth (Chaetodontidae, Perciformes) and the relationship to feeding ecology. Can J Zool 65:106–112.

Motta PJ, Hueter RE, Tricas TC. 1991. An electromyographic analysis of the biting mechanism of the lemon shark, *Negaprion brevirostris* — functional and evolutionary implications. J Morphol 210:55–69.

Motta PJ, Tricas TC, Hueter RE, Summers AP. 1997. Feeding mechanism and functional morphology of the jaws of the lemon shark *Negaprion brevirostris* (Chondrichthyes, Carcharhinidae). J Exp Biol 200:2765–2780.

Nishida K. 1990. Phylogeny of the suborder myliobatidoidei. Mem Fac Fish Hokk Univ 37:1–108.

Norton SF. 1988. Role of the gastropod shell and operculum in inhibiting predation by fishes. Science 241:92–94.

Ørvig T. 1951. Histologic studies of Placoderm and fossil elasmobranchs. I. The endoskeleton, with remarks on the hard tissues of lower vertebrates in general. Arkiv Zool 2:321–454.

Ørvig T. 1968. Current problems of lower vertebrate phylogeny. Proceeding of the fourth Nobel Symposium held in June 1967 at the Swedish Museum of Natural History (Naturhistoriska riksmuseet) in Stockholm. Stockholm: Almqvist and Wiksell.

Rasmussen E, Heard RW. 1995. Observations on extant populations of the softshell clam, *Mya arenaria* Linne, 1758 (Bivalvia: Myidae), from Georgia (USA) estuarine habitats. Gulf Res Rep 9:85–96.

Rensberger JM, Stefen C. 1995. Enamel specialization in hyenas: a structure useful for assessing bone-eating behavior in carnivorous mammals. J Vert Paleontol 15:49A.

Romer AS. 1964. The braincase of the Paleozoic elasmobranch *Tamiobatis*. Bull Mus Comp Zool 131:90–105.

Schaeffer B. 1981. The xenacanth neurocranium, with comments on elasmobranch monophyly. Bull Am Mus Nat Hist 169:1–66.

Schwartz FJ. 1965. Inter-American migrations and systematics of the western Atlantic cownose ray, *Rhinoptera bonasus*. Report of the Association of Island Marine Laboratories of the Caribbean (6th Meeting).

Smith BG. 1942. The heterodontid sharks: their natural history, and the external development of *Heterodontus japonicus* based on notes and drawings by Bashford Dean. In: Gudger EW, editor. The Bashford Dean memorial volume — archaic fishes. New York: American Museum of Natural History. p 651–769.

Smith MM, Hall BK. 1990. Development and evolutionary origins of vertebrate skeletogenic and odontogenic tissues. Biol Rev 65:277–373.

Summers AP. 1995. Is there really asymmetry in the muscle activation patterns of skates? (Abstract). Copeia 1995.

Summers AP, Koob TJ, Brainerd EL. 1998. Stingray jaws strut their stuff. Nature 395:450–451.

Swartz SM, Parker A, Huo C. 1998. Theoretical and empirical scaling patterns and topological homology in bone trabeculae. J Exp Biol 201:573–590.

Thompson DAW. 1917. On growth and form. London: Cambridge University Press.

Turingan RG, Wainwright PC. 1993. Morphological and functional bases of durophagy in the Queen Triggerfish, *Balistes vetula* (Pisces, Tetraodontiformes). J Morphol 215:101–118.

Wainwright PC. 1987. Biomechanical limits to ecological performance: mollusc-crushing by the Caribbean hogfish, *Lachnolaimus maximus* (labridae). J Zool 213:283–297.

Wainwright PC. 1988. Morphology and ecology: functional basis of feeding constraints in Caribbean labrid fishes. Ecology 69: 635–645.

Wallace JH. 1967. The batoid fishes of the East Coast of South Africa. II. Manta, eagle, duckbill cownose, butterfly and stingrays. South African Association for Marine Biological Research Investigational Report 16:1–56.

Wilga CD, Motta PJ. 1998. Conservation and variation in the feeding mechanism of the spiny dogfish *Squalus acanthias*. J Exp Biol 201:1345–1358.

Withers PC. 1992. Comparative animal physiology. New York: Saunders.